

# Narrowband Emission in Thomson Sources Operating in the High-Field Regime

Balša Terzić,<sup>1,2</sup> Kirsten Deitrick,<sup>2</sup> Alicia S. Hoffer,<sup>1</sup> and Geoffrey A. Krafft<sup>1,2</sup>

<sup>1</sup>*Jefferson Lab, Newport News, Virginia 23606, USA*

<sup>2</sup>*Center for Accelerator Studies, Old Dominion University, Norfolk, Virginia 23539, USA*

We present a novel and quite general analysis of the interaction of a high-field chirped laser pulse and a relativistic electron, in which exquisite control of the spectral brilliance of the upshifted Thomson-scattered photon is shown to be possible. Normally, when Thomson scattering occurs at high field strengths, there is ponderomotive line broadening in the scattered radiation. This effect makes the bandwidth too large for some applications and reduces the spectral brilliance. We show that such broadening can be corrected and eliminated by suitable frequency modulation of the incident laser pulse. Further, we suggest a practical realization of this compensation idea in terms of a chirped-beam driven free electron laser oscillator configuration and show that significant compensation can occur, even with the imperfect matching to be expected in these conditions.

PACS numbers: 29.20.Ej, 29.25.Bx, 29.27.Bd, 07.85.Fv

Sources of electromagnetic radiation relying upon Thomson scattering are increasingly being applied in fundamental physics research [1], and compact accelerator-based sources specifically designed for potential user facilities have been built [2]. One remarkable feature of the radiation emerging from such sources, compared to bremsstrahlung sources, is the narrowband nature of the radiation produced. For example, applications to X-ray structure determination [3], dark-field imaging [4, 5], phase contrast imaging [6], and computed tomography [7] have been demonstrated experimentally and take full advantage of the narrow bandwidth of the Thomson source.

Given that narrow bandwidth is desired, it is important to know and understand the sources of bandwidth of the scattered radiation and the limitations imposed on the performance of Thomson sources. For applications where the normalized vector potential of the incident laser pulse is much less than one (the low-field regime), the line width of the radiation from a scattering event reproduces the line width of the incident laser pulse. Unfortunately, when the normalized vector potential increases, as is desired for stronger sources, a detuning red-shift arises during the scattering events that tends to spread out the spectrum [8–10]. Physically, the scattering electron slows down, by a varying amount, as the incident pulse is traversed.

In a recent paper, Ghebreziabher, Shadwick, and Umstadter (GSU) observed that frequency modulation (FM), or “chirping”, of the scattering laser pulse can compensate for such ponderomotive line broadening, and suggested a form for this modulation [11]. Motivated by their observation, we present the exact analytic solution for optimal FM, recovering the low-field linewidth even in the high-field regime. The narrowing of the scattered pulse is Fourier-limited only by the duration of the incident pulse.

The essence of laser pulse chirping is analogous to free electron laser (FEL) undulator tapering [12–16]. In tapering, as deceleration occurs due to the FEL emis-

sion, the field strength is adjusted to preserve the same FEL emission frequency. To apply this idea to Thomson sources, the field strength dependence of the frequency shift must be countered by modulating the incident laser pulse. We show below how such modulation is straightforwardly accomplished in FEL oscillator lasers using the natural energy phase space curvature implicit in a bunch placed on the crest of an RF accelerating wave (Fig. 1).

In this Letter, we derive a prescription for calculating the choice of the FM that compensates the frequency spreading and recovers the initial spectral width. Even at high field strength, one can by proper choice of FM reduce the spectral width to the Fourier limit provided by the laser pulse width. Strictly speaking, the calculations in this Letter apply to Compton scattering only in the Thomson limit [1], i.e., when electron recoil may be neglected. This approximation is valid for Compton sources of X-rays originating from electron beams up to 100 MeV beam energy.

We report on calculations completed using the formalism developed in Ref. [9], which derives far-field spectral distribution of photons Thomson-scattered by a single electron. The incident laser pulse is described by a plane wave. This treatment is fully relativistic and includes the classical electron motion without approximation. We assume a linearly polarized incident plane wave described by a single component for the normalized vector potential  $\tilde{A}(\xi) = eA(\xi)/mc = a(\xi) \cos(2\pi\xi f(\xi)/\lambda)$ , where  $a(\xi)$  describes the envelope of the oscillation,  $\xi = z + ct$  is the coordinate giving distance along the laser pulse,  $f(\xi)$  specifies the laser FM, and  $\lambda$  is a convenient normalizing wavelength for the incident plane wave. In previous literature  $f(\xi) = 1$ , but following Ref. [11] we allow the possibility of laser chirping and let  $f$  vary throughout the pulse. Without loss of generality and for convenience of presentation, we require  $f(0) = 1$  for the peak amplitude centered at  $\xi = 0$ . Under this convention the calculated spectrum in the forward direction has a maximum near the frequency  $\omega_{max} \approx 2\pi c(1 + \beta)^2 \gamma^2 / [\lambda(1 + a^2(0)/2)]$ ,

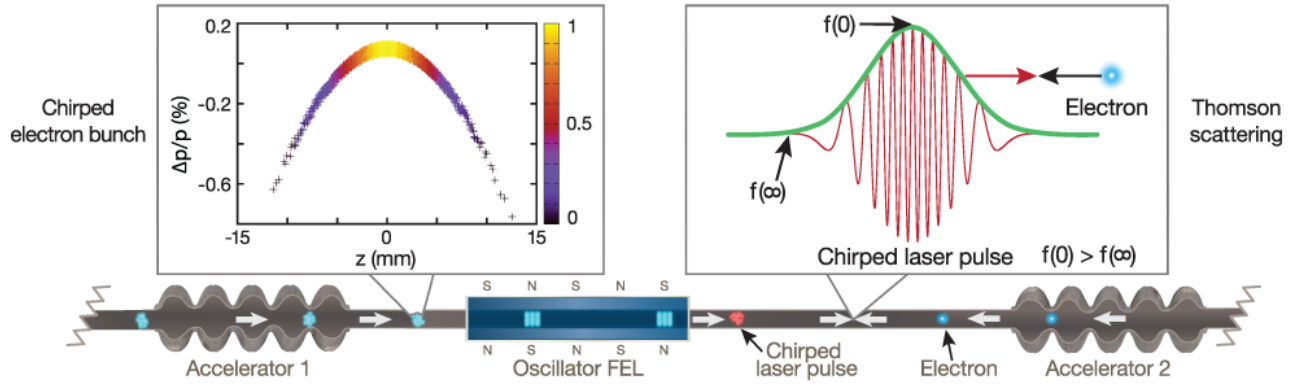


FIG. 1: Thomson scattering for a chirped laser pulse. Chirping the electron bunch before it passes through an oscillator FEL produces a chirped laser pulse. Thomson scattering occurs as the laser pulse collides with an electron. Narrowband emission of the resulting backscattered radiation is recovered through frequency chirping.

where  $\beta$  and  $\gamma$  are the usual relativistic factors for the scattering electron. We follow the practice in Ref. [9] and normalize frequencies by  $\omega_0 = (1 + \beta)^2 \gamma^2 2\pi c / \lambda$ . We report calculated spectra normalized by  $(d^2 E / d\omega d\Omega)_n = (1 + \beta)^2 \gamma r_e E_{beam} / c$  where  $r_e$  is the classical electron radius and  $E_{beam}$  is the total relativistic energy in a single electron. These spectra include both positive and negative frequency contributions in a single positive frequency spectrum. This normalization reflects the main beam energy dependence of the spectrum.

Because the longitudinal velocity of the electron changes and there is relativistic red-shifting during the laser pulse as the electron traverses it, the emitted spectrum of scattered radiation for a constant wavelength incident laser pulse is spread out beyond the spectral width of the incident pulse. Within each harmonic  $n$  in the emitted spectrum of scattered radiation, subsidiary peaks are featured whose number  $N_\tau$  is proportional to the field strength squared and the temporal duration of the pulse  $T$ . We use the Eq. (31) of [8] and a stationary phase argument [8, 17] to derive the exact relationship

$$N_\tau = (2n - 1) \frac{c}{\lambda} T \int_0^\infty a^2(\bar{\xi}) d\bar{\xi}, \quad (1)$$

where  $\bar{\xi} \equiv \xi / (\sqrt{2}\sigma)$ , with  $\sigma$  the pulse length. For a gaussian envelope  $a(\xi) = a_0 \exp[-\xi^2 / (2\sigma^2)]$  and  $n = 1$ ,  $N_\tau = \sqrt{2\pi} c T a^2(0) / 4\lambda$ , which agrees well with the empirical formula  $N_\tau \approx 0.24 T [\text{fs}] a^2(0)$  from Ref. [18]. While their empirical formula applies only to pulses with gaussian envelopes at  $\lambda = 800$  nm, ours is exact and valid for arbitrary envelope functions and wavelengths.

Our calculations were motivated by the suggestion in Ref. [11]. FM corresponding to their proposed  $\omega(t) = 2\omega_0 \left\{ 1 + [a(t) / \sqrt{2}a_0]^2 \right\} / 3$  (found in the text below their

Eq. (4)) is

$$f(\xi) = \frac{2}{3} \left( 1 + \frac{a^2(\xi)}{2a^2(0)} \right). \quad (2)$$

As understood and discussed subsequently, this substitution is strictly valid only when  $(\xi f(\xi))' = f(\xi) + \xi f'(\xi) \approx f(\xi)$ , that is, the FM occurs slowly enough. We also calculated the spectral distributions resulting from

$$f(\xi) = \sqrt{\frac{1 + a^2(\xi)/2}{1 + a^2(0)/2}}. \quad (3)$$

From Fig. 2(a), it is evident that the calculated spectrum for Eq. (3) represents a significant improvement over the non-modulated case. Because all harmonics improved, we concluded that a prescription exists to compensate all harmonics. Next, we investigated optimal configurations for  $f(\xi)$  using genetic optimization [19–23]. The optimization simultaneously maximized the height and minimized the width of the fundamental peak in the spectrum for a two-parameter family of functions of the form  $f_{GA}(\bar{\xi}; b, c) = c / [1 - (1 - c) \exp(-b\bar{\xi}^2)]$ . The best result has  $b = 0.859$  and  $c = 0.907$ . The spectrum of the optimal  $f_{GA}$ , as well as the exact FM derived below is also shown in Fig. 2(a). Genetic optimization performs quite well, as the spectrum of the optimal  $f_{GA}$  is very close to that of the exact FM.

We investigated the dependence of the optimal parameters of  $f_{GA}$  on the field strength in the incident laser pulse and observed that  $c$  scaled directly as  $a(0)^2 / 4$ . Convinced that such simple scaling indicates an underlying physics cause for narrowband emission, we derived the following analytical condition that leads to minimal emission bandwidth.

For incident laser pulses of the given form and when  $f(\xi)$  is not slowly varying, one must define *local* values of

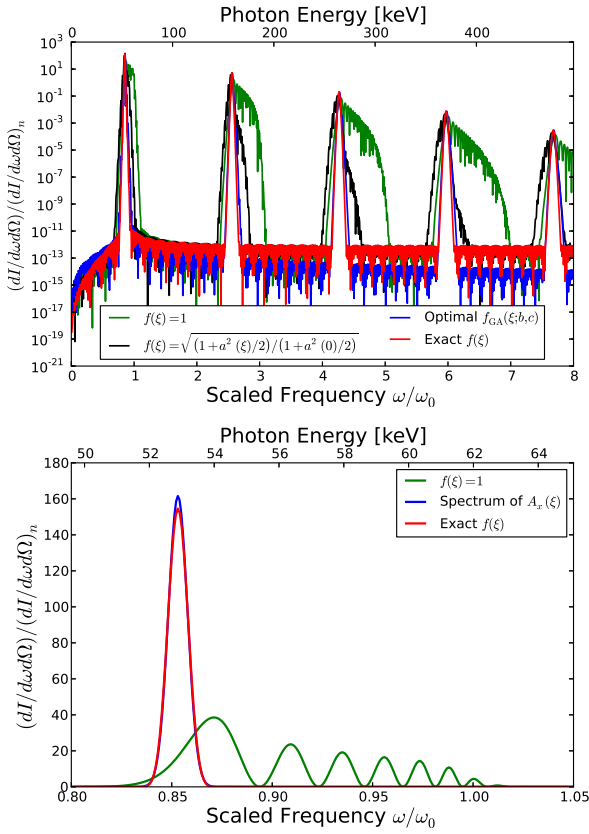


FIG. 2: Top: Normalized spectra of scattered radiation for the case without FM (green line), FM from Eq. (3) (black line), FM from optimal  $f_{GA}(\xi; b, c)$  (blue line), and the exact FM from Eq. (4) (red line). The shapes of the spectra — both non-modulated and modulated — are independent on the scattering electron’s energy. Bottom: Complete correction of spectral width is demonstrated by this comparison of the case with no FM (green line), the Fourier transform of the amplitude function (blue line), and the case with exact FM (red line). In both panels, a gaussian envelope is used with  $a_0 = 0.587$  and electron’s  $\gamma = 100$  as in Fig. 2 of [9].

the pulse frequency and wave number as

$$\omega(\xi) = \partial\Phi/\partial t = cd\Phi/d\xi, \quad k(\xi) = \partial\Phi/\partial z = d\Phi/d\xi,$$

where  $\Phi$  is the incident wave phase. Lorentz-transforming these quantities into the beam frame (frame with zero average beam velocity) yields  $\omega' = \frac{(1+\beta^*)\gamma^*\omega}{\sqrt{1+a(\xi)^2/2}}$  and  $k' = (1+\beta^*)\gamma^*k$ , where  $\gamma^*(\xi) = \gamma/\sqrt{1+a(\xi)^2/2}$  and  $\beta^*(\xi) = \sqrt{1-(1/\gamma^2)(1+a(\xi)^2/2)}$  are local values within the pulse. To minimize the spectral width in the lab frame one should arrange the frequency in the beam frame to emit radiation Doppler-shifted back to a constant frequency in the lab frame. Thus for all  $\xi$ -values we require *locally*

$$(1+\beta^*)^2\gamma^{*2}d\Phi/d\xi = C = (1+\beta)^2\gamma^2d\Phi/d\xi(\xi = -\infty),$$

for some constant  $C$ . This exact case is found by inte-

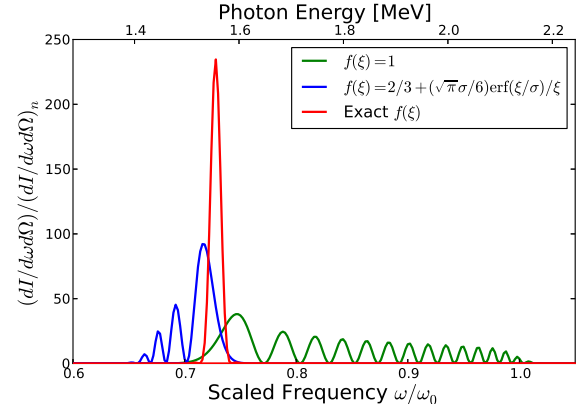


FIG. 3: Narrowing the radiation spectra by exact FM. Scattered spectral distributions calculated with no FM (green line), the GSU FM as in Eq. (5) (blue line), and the exact FM given in Eq. (6) (red line). A gaussian envelope is used with  $a_0 = 0.865$  as in Fig. 6 of [11]. Note the linear scale and that only data in the first harmonic is displayed for both panels. The top  $x$ -axes in both panels denote photon energies for the case of  $E_{beam} = 300$  MeV,  $\lambda = 800$  nm, FWHM pulse duration of 90 fs, as in Fig. 6 of [11].

gration

$$\frac{d}{d\xi} [\xi f(\xi)] = (1+a(\xi)^2/2)f(\xi = -\infty),$$

as both  $\beta$  and  $\beta^*$  are close to one for relativistic scattering. The solution with the boundary condition  $f(0) = 1$  is

$$f(\xi) = \frac{1}{1+a(0)^2/2} \left( 1 + \frac{\int_0^\xi a(\xi')^2 d\xi'}{2\xi} \right). \quad (4)$$

Clearly, this function falls from 1 to the constant value  $f(\pm\infty) = (1+a(0)^2/2)^{-1}$ . This characteristic, that  $f$  falls off to the same value at  $\xi = \pm\infty$ , is shared by any single-peaked symmetrical model for the amplitude function, as is clear from the general formula in Eq. (4). We can now explain the scaling in the optimization. The optimal  $f_{GA}$  closely traces the exact FM around  $\xi = 0$ , while its purely exponential tails are unable to match the exact  $1/\xi$  behavior.

Applying this pulse-chirping prescription leads to narrowband emission, as shown in Fig. 2(a). The non-FM case clearly shows ponderomotive broadening at high field strength that is corrected away using the exact FM prescription. Notice a non-trivial conclusion of this calculation: our prescription works across all the harmonics shown, whereas Ref. [11] presents information on the fundamental line only. Additionally, because Eq. (4) is energy-independent, compensation occurs for all electrons in a bunch of electrons with varying energy. In this case, the linewidth is spread in the usual way by the energy spread [1].

In Fig. 2(b) we compare the spectral peak in the high-field case with the spectrum obtained simply from the Fourier transform of the gaussian amplitude/envelope function  $a(\xi)$ , suitably shifted to the peak frequency of the first curve. Observe that the corrected width is identical to that generated by the gaussian (and is Fourier-limited by the duration of the scattered pulse). One cannot expect to obtain a peak narrower than the Fourier-limited linewidth. The scattered photons in the high-field case have a linewidth much narrower than that of the Fourier spectrum of the incident frequency-modulated laser pulse.

Using this more accurate method defining the frequency and wave number, it is now possible to generate a scattered distribution closer to the one reported in Ref. [11]. Integrating

$$\frac{d}{d\xi} [\xi f_{\text{GSU}}(\xi)] = \frac{2}{3} \left( 1 + \frac{a(\xi)^2}{2a(0)^2} \right)$$

for a gaussian envelope yields the analogous  $f_{\text{GSU}}$  with the correct boundary conditions

$$f_{\text{GSU}}(\xi) = \frac{2}{3} \left( 1 + \frac{\sqrt{\pi}\sigma}{4\xi} \text{erf}(\xi/\sigma) \right). \quad (5)$$

For comparison, exact FM for the gaussian envelope is

$$f(\xi) = \frac{1}{1 + a_0^2/2} \left( 1 + \frac{\sqrt{\pi}\sigma a_0^2}{4\xi} \text{erf}(\xi/\sigma) \right). \quad (6)$$

FM obtained using the empirical prescription of [11], and given here in Eqns. (2) and (5), does not satisfy the asymptotic behavior of  $\lim_{a(0) \rightarrow 0} f(\xi) = 1$  because they do not even depend on  $a(0)$ . Therefore Eqn. (5) should not be directly compared to the exact FM in Eq. (6) which satisfies this asymptotic behavior. A cursory inspection shows that the empirical FM in Eq. (5) is equivalent to the exact FM in Eq. (6) for  $a(0) = 1$  and explains why [11] observed a substantial narrowing of the spectra for their case of  $a(0) = 0.865 \approx 1$ .

In Fig. 3 we show scattered spectral distributions calculated with  $f(\xi) = 1$ , the modified GSU model in Eq. (5), and the fully corrected result using Eq. (6), now on a linear scale as in the previous publication [24]. We observe that pulse chirping increases the peak spectral energy density by a factor of 2.4 in going from unmodulated to the Eq. (5) model, and another factor of 2.5 in applying the exact FM prescription.

Alternatively, Eq. (4) follows from a stationary phase analysis of [8, 9, 17]

$$\begin{aligned} D_x &= \int_{-\infty}^{\infty} \frac{d\xi}{\gamma(1+\beta)} \tilde{A}(\xi) \exp \left[ i\omega \left( \frac{\xi}{c\gamma^2(1+\beta)^2} + \frac{1}{c\gamma^2(1+\beta)^2} \int_{-\infty}^{\xi} \tilde{A}^2(\xi') d\xi' \right) \right] \\ &\approx \frac{1}{2} \int_{-\infty}^{\infty} \frac{d\xi}{\gamma(1+\beta)} a(\xi) \exp \left[ \frac{-2\pi i \xi f(\xi)}{\lambda} + i\omega \left( \frac{\xi}{c\gamma^2(1+\beta)^2} + \frac{1}{c\gamma^2(1+\beta)^2} \int_{-\infty}^{\xi} \tilde{A}^2(\xi') d\xi' \right) \right] \end{aligned} \quad (7)$$

where  $d^2 E/d\omega d\Omega = r_e E_{\text{beam}} \omega^2 |D_x|^2 / (4\pi^2 c^3 \gamma) = (d^2 E/d\omega d\Omega)_n (\omega/\omega_0)^2 |(1+\beta)\gamma D_x/\lambda|^2$  in the forward direction. The dominant contribution to  $D_x$  comes from replacing  $\tilde{A}^2(\xi)$  by its average value  $a^2(\xi)/2$  in the phase integral. Applying Eq. (4) guarantees that the phase in the integral is constant on average and only slightly modulated as a function of  $\xi$ . Therefore, the maximum value of the amplitude of  $D_x$  is well-approximated by

$$|D_x|_{\text{max}} \approx \frac{1}{2\gamma(1+\beta)} \int_{-\infty}^{\infty} a(\xi) d\xi,$$

as observed in the exact FM case.

The fact that the  $f$  function falls from a maximum in the middle of the pulse, suggests an immediate practical realization of the frequency chirping. Suppose an FEL oscillator is constructed where the driving beam bunches

are long enough that the RF-curvature related energy spread is substantial (see Fig. 1). The frequency of the resulting laser pulse emitted by the oscillator FEL will also be chirped:

$$\omega(\xi) = \omega(\xi = 0) \cos^2(2\pi\xi/\lambda_{\text{RF}}),$$

where  $\lambda_{\text{RF}}$  is the wavelength of the RF accelerating wave, and it is assumed that the center of the electron pulse coincides with the accelerating wave maximum. The circulating bunches will generate a  $\xi$ -dependent frequency from the energy dependence of the FEL emission.

Using our prescription for defining  $f(\xi)$ ,

$$\frac{d}{d\xi} [\xi f_{\text{RF}}(\xi)] = \cos^2(2\pi\xi/\lambda_{\text{RF}})$$

yields

$$f_{\text{RF}}(\xi) = \frac{1}{2} + \frac{1}{\xi} \frac{\lambda_{\text{RF}}}{8\pi} \sin(4\pi\xi/\lambda_{\text{RF}}). \quad (8)$$

Notice the dependence has the correct sign to allow compensation. Expanding the above equation around the center of the pulse produces  $f_{\text{RF}}(\xi) \approx 1 - 4\pi^2\xi^2/(3\lambda_{\text{RF}}^2)$ , and matching it to the quadratic dependence of the exact FM function in Eq. (6) yields  $\lambda_{\text{RF}0} = \sqrt{8\pi} \frac{\sqrt{1+a_0^2/2}}{a_0} \sigma$ .

TABLE I: Peak height (normalized to peak height for exact FM) and optimal choice for  $\lambda_{\text{RF}}$  for each harmonic when approximated by RF waveform curvature model in Eq. (8).

Harmonic	Peak Height	$\lambda_{\text{RF}}/\lambda_{\text{RF}0}$
1	0.84	1.47
3	0.89	1.21
5	0.94	1.14
7	0.98	1.10
9	0.99	1.12

Because we cannot reproduce the optimal frequency profile exactly by these means, we investigated whether we could obtain peaks in the spectra of all reported harmonics close to those in the optimal case. Our results showing the spectral peak values and the optimal  $\lambda_{\text{RF}}$  for the various harmonics, compared to the optimal case, are reported in Table I. Indeed, we are able to get close-to-optimal performance across all harmonics with slight adjustments in RF-frequency (compressed bunch length in practice). Interestingly, higher harmonics achieved optimal performance by adjusting closer to the  $\lambda_{\text{RF}0}$  value.

Finally, we investigated the robustness of the solutions. Requiring the spectrum peaks to be degraded under 10% leads to a restriction of the bunch length. Because the peaks as a function of bunch length are quite broad, control of the bunch length at the 20% level is indicated. There is already experimental evidence [25] that controlled chirping of an electron bunch driving an FEL oscillator is reflected in the FEL output radiation characteristics.

The cases discussed in this paper, corresponding to laser parameters of interest in many sources, all yield less than one photon per electron. More quantitatively, from [1] we derive the domain of validity of the no-electron-recoil approximation, i.e. when the number of emitted photons  $n_\gamma = (\alpha\lambda)/(3\pi) \int_{-\infty}^{\infty} \left| \partial\tilde{A}(\xi)/\partial\xi \right|^2 d\xi < 1$ , to be for field strength  $a_0 < \sqrt{3\lambda/(2\pi^{1/2}\alpha\sigma)}$ , with  $\alpha$  the fine structure constant. For the cases considered here this restriction reduces to  $a_0 < 2.39$ , which is easily satisfied in the cases reported in this Letter ( $n_\gamma = 0.06$  for  $a_0 = 0.587$ ,  $\gamma = 100$  and  $n_\gamma = 0.13$  for  $a_0 = 0.865$ ,  $E_{\text{beam}} = 300$  MeV case). Therefore, the field strength

is not so large that quantum mechanical multi-photon emission processes need to be considered.

It is our belief that because including electron recoil in the formula for the emitted photon energy is straightforward, a calculation procedure similar to the above will lead to chirping prescriptions including the full Compton effect.

The calculations presented suggest the following conclusions. Frequency chirping of the incident laser pulse can indeed lead to bandwidth *reduction* in the radiation emerging from Thomson scattering events at high field strength, as suggested by GSU. This somewhat counter-intuitive situation arises because, with proper tuning, the double-Doppler-shifted frequency in the lab frame may be adjusted to a constant value by compensating the frequency shifts due to velocity changes against the FM. We have analytically derived exact frequency compensation functions that may be applied to very general longitudinal pulse shapes and across all the lower-order harmonics, which become more prominent in the high-field regime. We have suggested a practical realization of this compensation idea in terms of a chirped-beam driven FEL oscillator configuration and shown that significant compensation can occur, even with imperfect matching.

Discussions with S. Benson and D. Douglas are gratefully acknowledged, who assured us that FEL laser pulse chirping could be accomplished by electron beam chirping. S. Benson provided references on early work in FEL tapering. R. Ruth provided information on the work at Lyncean Technologies. In addition, fruitful interactions with I. Ghebregziabher and D. Umstadter are acknowledged. They graciously consented to our Fig. 3 as being reported as qualitatively and quantitatively similar to their Fig. 6 of Ref. [11], even though somewhat different models were used to generate the two figures. Our communications with G. P. Williams, M. Tiefenback and S. Corneliussen were very helpful. We are thankful to J. Griffin for her help in generating our Fig. 1. This Letter is authored by Jefferson Science Associates, LLC under U. S. Department of Energy (DOE) Contract No. DE-AC05-06OR23177. The U. S. Government retains a non-exclusive, paid-up, irrevocable, world-wide license to publish or reproduce this manuscript for U. S. Government purposes. K. D. is supported by DOE Contract No. de-sc00004094.

- 
- [1] G. A. Krafft and G. Priebe, *Rev. Accel. Sci. Tech.* **03**, 147 (2010).
  - [2] Z. Huang and R. Ruth, *Phys. Rev. Lett.* **80**, 976 (1998). See also [www.lynceantech.com](http://www.lynceantech.com).
  - [3] J. Abendroth *et al.*, *Journal of Structural and Functional Genomics* **11**, 91, (2010).
  - [4] M. Bech *et al.*, *Photon Lasers Med* **1**, 47 (2012).
  - [5] S. Schleele *et al.*, *Proc. Nat. Acad. Sci. USA* **109**, 17880

- (2012) [doi: 10.1073/pnas.1206684109]
- [6] M. Bech *et al.*, *J. Synchrotron Rad.* **16**, 43 (2009).
- [7] K. Achterhold *et al.*, *Sci. Rep.* **3**, 1313 (2013).
- [8] C. Brau, *Phys. Rev. ST-AB* **7**, 020701 (2004).
- [9] G. A. Krafft, *Phys. Rev. Lett.* **92**, 204802 (2004).
- [10] J. Gao, *Phys. Rev. Lett.* **93**, 243001 (2004).
- [11] I. Ghebregziabher, B. A. Shadwick, and D. Umstadter, *Phys. Rev. ST-AB* **16**, 030705 (2013). See also arXiv:1204.1068.
- [12] N. M. Kroll, P. L. Morton, and M. N. Rosenbluth, *IEEE Journal of Quantum Electronics* **QE-17**, 1436 (1981).
- [13] E. L. Saldin, E. A. Schneidmiller, and M. V. Yurkov, *Opt. Commun.*, **103**, 297 (1993).
- [14] J. A. Edighoffer *et al.* *Phys. Rev. Lett.* **52**, 344 (1984).
- [15] A. Christodoulou *et al.* *Phys. Rev. E* **66**, 056502 (2002).
- [16] T. J. Orzechowski *et al.* *Phys. Rev. Lett.* **57**, 344 (1986)
- [17] G. F. Carrier, M. Krook, and C. E. Pearson, *Functions of a Complex Variable*, Section 6-4, pgs. 272-275, (Hod Books, Ithaca, New York 1983).
- [18] T. Heinzl, D. Seipt, and B. Kämpfer, *Phys. Rev. A* **81**, 022125 (2010).
- [19] E. Zitzler, M. Laumanns, and L. Thiele, In *Evolutionary Methods for Design, Optimisation and Control with Application to Industrial Problems (EUROGEN 2001)*, edited by K. Giannakoglou, D. Tsahalis, J. Periaux, K. Papailiou & T. Fogarty, pgs. 95-100 (CIMNE, Athens, 2001).
- [20] S. Bleuler, M. Laumanns, L. Thiele, and E. Zitzler, *Tech. Rep. 154, Institut für Technische Informatik und Kommunikationsnetze*, (ETH Zürich, Zürich, 2002).
- [21] S. Bleuler, M. Laumanns, L. Thiele and E. Zitzler, in *Evolutionary Multi-Criterion Optimization (EMO 2003)*, edited by C. Fonseca, P. J. Fleming, E. Zitzler, K. Deb, and L. Thiele, pgs. 494-508 (Springer, Berlin, 2003).
- [22] I. Bazarov and C. Sinclair, *Phys. Rev. ST-AB* **8**, 034202 (2005).
- [23] A. Hoffer *et al.*, *Phys. Rev. ST-AB* **16**, 010101 (2013).
- [24] Compare with Fig. 6 of Ref. [11] or Fig. 3 in the archive version. We shared the results of our calculations with these authors, who have separately confirmed the qualitative and quantitative agreement between this model and their results.
- [25] S. Zhang, S. Benson, D. Douglas, G. Neil, and M. Shinn, *Proc. FEL2009*, Liverpool, UK, pgs. 211-214 (2009).